

Dear Author,

Here are the proofs of your article.

- You can submit your corrections **online**, via **e-mail** or by **fax**.
- For **online** submission please insert your corrections in the online correction form. Always indicate the line number to which the correction refers.
- You can also insert your corrections in the proof PDF and **email** the annotated PDF.
- For fax submission, please ensure that your corrections are clearly legible. Use a fine black pen and write the correction in the margin, not too close to the edge of the page.
- Remember to note the **journal title**, **article number**, and **your name** when sending your response via e-mail or fax.
- **Check** the metadata sheet to make sure that the header information, especially author names and the corresponding affiliations are correctly shown.
- **Check** the questions that may have arisen during copy editing and insert your answers/ corrections.
- **Check** that the text is complete and that all figures, tables and their legends are included. Also check the accuracy of special characters, equations, and electronic supplementary material if applicable. If necessary refer to the *Edited manuscript*.
- The publication of inaccurate data such as dosages and units can have serious consequences. Please take particular care that all such details are correct.
- Please **do not** make changes that involve only matters of style. We have generally introduced forms that follow the journal's style. Substantial changes in content, e.g., new results, corrected values, title and authorship are not allowed without the approval of the responsible editor. In such a case, please contact the Editorial Office and return his/her consent together with the proof.
- If we do not receive your corrections **within 48 hours**, we will send you a reminder.
- Your article will be published **Online First** approximately one week after receipt of your corrected proofs. This is the **official first publication** citable with the DOI. **Further changes are, therefore, not possible.**
- The **printed version** will follow in a forthcoming issue.

Please note

After online publication, subscribers (personal/institutional) to this journal will have access to the complete article via the DOI using the URL: [http://dx.doi.org/\[DOI\]](http://dx.doi.org/[DOI]).

If you would like to know when your article has been published online, take advantage of our free alert service. For registration and further information go to: <http://www.link.springer.com>.

Due to the electronic nature of the procedure, the manuscript and the original figures will only be returned to you on special request. When you return your corrections, please inform us if you would like to have these documents returned.

Metadata of the article that will be visualized in OnlineFirst

Please note: Images will appear in color online but will be printed in black and white.

ArticleTitle	A mathematical method for parameter estimation in a tumor growth model	
Article Sub-Title		
Article CopyRight	SBMAC - Sociedade Brasileira de Matemática Aplicada e Computacional (This will be the copyright line in the final PDF)	
Journal Name	Computational and Applied Mathematics	
Corresponding Author	Family Name	Fernández
	Particle	
	Given Name	D.
	Suffix	
	Division	Facultad de Matemática, Astronomía y Física
	Organization	Universidad Nacional de Córdoba, CIEM-CONICET
	Address	Medina Allende s/n, Ciudad Universitaria, 5000, Córdoba, Argentina
	Email	dfernandez@famaf.unc.edu.ar
Author	Family Name	Knopoff
	Particle	
	Given Name	D.
	Suffix	
	Division	Dipartimento di Scienze Matematiche
	Organization	Politecnico di Torino
	Address	Corso Duca degli Abruzzi 24, 10100, Torino, Italia
	Division	Facultad de Matemática, Astronomía y Física
	Organization	Universidad Nacional de Córdoba, CIEM-CONICET
	Address	Medina Allende s/n, Ciudad Universitaria, 5000, Córdoba, Argentina
	Email	knopoff@famaf.unc.edu.ar
Author	Family Name	Torres
	Particle	
	Given Name	G.
	Suffix	
	Division	Facultad de Matemática, Astronomía y Física
	Organization	Universidad Nacional de Córdoba, CIEM-CONICET
	Address	Medina Allende s/n, Ciudad Universitaria, 5000, Córdoba, Argentina
	Email	torres@famaf.unc.edu.ar
Author	Family Name	Turner
	Particle	
	Given Name	C.
	Suffix	
	Division	Facultad de Matemática, Astronomía y Física
	Organization	Universidad Nacional de Córdoba, CIEM-CONICET
	Address	Medina Allende s/n, Ciudad Universitaria, 5000, Córdoba, Argentina

	Email	turner@famaf.unc.edu.ar
Schedule	Received	10 December 2013
	Revised	20 April 2015
	Accepted	7 July 2015
Abstract	<p>In this paper, we present a methodology for estimating the effectiveness of a drug, an unknown parameter that appears on an avascular, spheric tumor growth model formulated in terms of a coupled system of partial differential equations (PDEs). This model is formulated considering a continuum of live cells that grow by the action of a nutrient. Volume changes occur due to cell birth and death, describing a velocity field. The model assumes that when the drug is applied externally, it diffuses and kills cells. The effectiveness of the drug is obtained by solving an inverse problem which is a PDE-constrained optimization problem. We define suitable objective functions by fitting the modeled and the observed tumor radius and the inverse problem is solved numerically using a Pattern Search method. It is observed that the effectiveness of the drug is retrieved with a reasonable accuracy. Experiments with noised data are also considered and the results are compared and contrasted.</p>	
Keywords (separated by '-')	Avascular tumor - PDE-constrained optimization - Inverse problem - Mathematical modeling	
Mathematics Subject Classification (separated by '-')	35R30 - 65M32 - 35Q80	
Footnote Information	<p>Communicated by George S. Dulikravich. This work has been partially supported by the European Union FP7 Health Research Grant No. FP7-HEALTH-F4-2008-202047-RESOLVE, and ANPCyT, CONICET and SECyT-UNC.</p>	

A mathematical method for parameter estimation in a tumor growth model

D. Knopoff^{1,2} · D. Fernández² · G. Torres² ·
C. Turner²

Received: 10 December 2013 / Revised: 20 April 2015 / Accepted: 7 July 2015
© SBMAC - Sociedade Brasileira de Matemática Aplicada e Computacional 2015

Abstract In this paper, we present a methodology for estimating the effectiveness of a drug, an unknown parameter that appears on an avascular, spheric tumor growth model formulated in terms of a coupled system of partial differential equations (PDEs). This model is formulated considering a continuum of live cells that grow by the action of a nutrient. Volume changes occur due to cell birth and death, describing a velocity field. The model assumes that when the drug is applied externally, it diffuses and kills cells. The effectiveness of the drug is obtained by solving an inverse problem which is a PDE-constrained optimization problem. We define suitable objective functions by fitting the modeled and the observed tumor radius and the inverse problem is solved numerically using a Pattern Search method. It is observed that the effectiveness of the drug is retrieved with a reasonable accuracy. Experiments with noised data are also considered and the results are compared and contrasted.

Communicated by George S. Dulikravich.

This work has been partially supported by the European Union FP7 Health Research Grant No. FP7-HEALTH-F4-2008-202047-RESOLVE, and ANPCyT, CONICET and SECyT-UNC.

✉ D. Fernández
dfernandez@famaf.unc.edu.ar

D. Knopoff
knopoff@famaf.unc.edu.ar

G. Torres
torres@famaf.unc.edu.ar

C. Turner
turner@famaf.unc.edu.ar

¹ Dipartimento di Scienze Matematiche, Politecnico di Torino, Corso Duca degli Abruzzi 24, 10100 Torino, Italia

² Facultad de Matemática, Astronomía y Física, Universidad Nacional de Córdoba, CIEM-CONICET, Medina Allende s/n, Ciudad Universitaria, 5000 Córdoba, Argentina

12 **Keywords** Avascular tumor · PDE-constrained optimization · Inverse problem ·
 13 Mathematical modeling

14 **Mathematics Subject Classification** 35R30 · 65M32 · 35Q80

15 1 Introduction

16 The scientific community agrees that mathematical modeling of tumor growth is an effective and important step in promoting knowledge about cancer, becoming one of the most studied topics in mathematical biology. Pioneer models for tumor growth were proposed by Adam (1986) and Greenspan (1972). Some developments in the last years include, among many others, cell-focused (Rejniak and McCawley 2010), hybrid (Preziosi and Vitale 2011) and continuum models (Wise et al. 2008), each of them with some specific fields of applications. In (Byrne and Drasdo 2009), a comparison between them is considered. Some important contributions in the field include models based on the diffusion of nutrients taking into account the physiological changes accompanying the growth of avascular tumors (Kiran et al. 2009), those regarding to biological motivations for in silico models of cancer (Edelman et al. 2010), multi-phase models regarding thermodynamic equilibrium (Grillo et al. 2009), and the recent Bayesian approach for selecting and validating mathematical and computational models (Oden et al. 2013). The recent papers (Bellomo et al. 2008; Tracqui 2009; Lowengrub et al. 2010; Roose et al. 2007) are valuable reviews and the interested reader is referred to them for additional useful references.

32 The advantages of continuum models are that they are understandable, tractable to mathematical analysis and intuitive from biological principles. They contain a few parameters and can use laws from physics. On the other hand, the advantages of discrete models are able to work in other scales and each cell can be treated independently with no extra complication (Roose et al. 2007).

37 In this present paper, we focus on the growth of a multicellular spheroid (MCS) (Hamilton 1998). A MCS is a cluster of cancer cells grown in vitro to mimic the early stages of in vivo avascular tumor growth. In fact, in vitro observations (Sutherland 1988) suggest that in the early stages solid tumors remain approximately spherical as they grow, possessing a central core of necrotic cells, with proliferating cells restricted to the outer rim of the tumor.

42 Since this model considers the evolution of a system from a single progenitor cell to $\mathcal{O}(10^6)$ cells in vitro, the continuum approach is better than an agent-based approach (Byrne and Drasdo 2009).

45 Mathematical models of MCSs are typically continuous models which consist of an ordinary differential equation (ODE) representing the evolution of the outer tumor boundary, and a set of partial differential equations (PDEs) describing, for example, the distribution within the tumor of vital nutrients, such as oxygen and glucose, and growth inhibitors (Byrne and Chaplain 1997). That is why in this general approach of modeling, the key variables are the tumor size, e.g., tumor radius, and the concentration of the aforementioned substances. Since the tumor changes in size over time, the domain on which the models are formulated must be determined as part of the solution process, giving a vast class of moving boundary problems (Byrne and Chaplain 1997; Crank 1984).

54 In this article, we propose a framework for estimating an unknown parameter via PDE-constrained optimization, following a model by Ward and King (2003), which is a two-phase model with the two phases being live cells and dead cells.

In this approach, avascular tumor growth is modeled via a coupled nonlinear system of PDEs, making its numerical solution quite challenging. It is worth mentioning that all tumor growth models involve a certain number of parameters (Hogea et al. 2008), and that some of them are difficult to obtain experimentally. In particular, we will consider a parameter that represents the effectiveness of a chemotherapeutic drug, because it encapsulates both the drug degradation rate and the diffusivity, and it is consequently a key parameter in determining the success of the drug (Ward and King 2003). In addition, according to the definition given in (Ward and King 2003), the drug penetration depth within the tumor can be shown to be proportional to the square root of this parameter.

To obtain the effectiveness of the drug, we define a function to be minimized that establishes a comparison between the measured radius of the tumor and the one predicted by the model. We observe that the evolution of the radius of the MCSs is in fact a measurable variable. For instance, in (Monazzam et al. 2007; Bergstrom et al. 2008; Herrmann et al. 2008), special procedures were used to evaluate tumor growth and quantify its radius.

This kind of problem constitutes a particular application of the so-called inverse problems, which are being increasingly used in a broad number of fields in applied sciences. For instance, problems referred to structured population dynamics (Perthame and Zubelli 2007), computerized tomography and image reconstruction in medical imaging (van den Doel et al. 2011; Zubelli et al. 2003), and more specifically tumor growth (Knopoff et al. 2013; Agnelli et al. 2011; Hogea et al. 2008), among many others. An inverse problem assumes a direct problem that is a well-posed problem of mathematical physics. In other words, if we know completely a physical model, we have a classical mathematical description of it. But if one of the parameters describing this model is to be found (from additional boundary/experimental data), then we arrive at an inverse problem.

The paper is organized as follows. Section 2 introduces the avascular tumor growth model. Section 3 presents a numerical scheme for solving the system of PDEs. Section 4 formulates the inverse problem, defining the functions to be minimized. Section 5 is dedicated to the numerical experiments and the discussion of the results. Finally, conclusions are given in Sect. 6.

2 Mathematical model

We consider the model proposed by (Ward and King 2003). The tumor is a spheroid which consists of a continuum of living cells, in one of two states: live or dead. The birth and death rates depend on the nutrient and chemotherapeutic drug concentrations. It is supposed that those processes generate volume changes, leading to cell movement described by a velocity field. Assuming spherical symmetry, the system of equations to be studied is:

$$\frac{\partial n}{\partial \tau} + \frac{1}{r^2} \frac{\partial (r^2 v n)}{\partial r} = [k_m(c) - k_d(c) - K G(k_m(c)) w] n, \quad (1)$$

$$\frac{\partial c}{\partial \tau} + \frac{1}{r^2} \frac{\partial (r^2 v c)}{\partial r} = \frac{D}{r^2} \frac{\partial}{\partial r} \left(r^2 \frac{\partial c}{\partial r} \right) - \beta k_m(c) n, \quad (2)$$

$$\frac{1}{r^2} \frac{\partial (r^2 v)}{\partial r} = [V_L k_m(c) - (V_L - V_D) \{k_d(c) + K G(k_m(c)) w\}] n, \quad (3)$$

$$\frac{\partial w}{\partial \tau} + \frac{1}{r^2} \frac{\partial (r^2 v w)}{\partial r} = \frac{D_w}{r^2} \frac{\partial}{\partial r} \left(r^2 \frac{\partial w}{\partial r} \right) - \frac{K}{\omega} G(k_m(c)) w n, \quad (4)$$

Table 1 Summary of model variables and symbols

Variable	Dimensionless variable	Description
r	y	Spatial independent variable
τ	t	Temporal independent variable
n	N	Live cell density
c	C	Nutrient concentration
v	V	Velocity field
w	W	Drug concentration
s	S	Tumor radius

where the independent variables are the radial position r inside the tumor and time τ and the dependent variables n , c , v and w are the live cell density (cells/unit volume), nutrient concentration, velocity and drug concentration, respectively. A summary of model variables is included in Table 1 at the end of this Section. As it is described in (Ward and King 2003), Eq. (1) states that the rate of change of n is dependent on the difference between the birth rate $k_m(c)$, and the death rate, which can be either natural at a rate $k_d(c)$ [as described in (Ward and King 1997)] or due to drug effects, at a rate $KG(k_m(c))w$. The functions k_m and k_d are taken to be generalized Michaelis–Menten kinetics with exponent 1, i.e.,

$$k_m(c) = A \left(\frac{c}{c_c + c} \right), \quad k_d(c) = B \left(1 - \sigma \frac{c}{c_d + c} \right). \quad (5)$$

where A and B are the maximum birth and death rates theoretically attainable when c tends to infinity and $c = 0$, respectively, the constants c_c and c_d are the standard half-saturation concentrations in the Michaelis–Menten terms, and $B(1 - \sigma)$ is the minimum death rate attainable when the concentration tends to infinity with $0 \leq \sigma \leq 1$. The constant K is the maximum possible rate of drug-induced cell death and G is a function that represents the dependence between drug action and cell cycle.

Equation (2) states that the nutrient is consumed at a rate proportional (with constant of proportionality equal to β) to the rate of mitosis, and its diffusion is described by the Fick's law with the diffusion coefficient D taken to be constant since spheroid's heterogeneity does not significantly affect diffusion rates.

Equation (3) states that the rate of volume change is given by the difference in volume generated via birth from that lost by death (it is assumed that a live cell occupies a volume V_L that is twice the volume of a death cell V_D).

The diffusion of the drug is also described by Fick's law (with diffusion coefficient D_w), and it is assumed that it is degraded only when it attacks a living cell, giving a maximum degradation rate K/ω . The constant ω can be interpreted as a measure of the drug's effectiveness, as explained in (Ward and King 2003), with increasing ω implying that less drug is consumed to produce the same effects during the killing process. These considerations lead to Eq. (4). An important consequence of knowing ω is that it let us compute the drug penetration depth $\sqrt{\omega D_w V_L / K}$.

Since the tumor radius changes over time, the domain on which the model is formulated must be determined as part of the solution. Let $s(\tau)$ be the tumor radius at time τ . Let us suppose that at time $\tau = 0$ the tumor has a radius s_I and a living cell density $n_I(r)$. The initial conditions on c and w are not necessary under the quasi-steady assumptions. Then

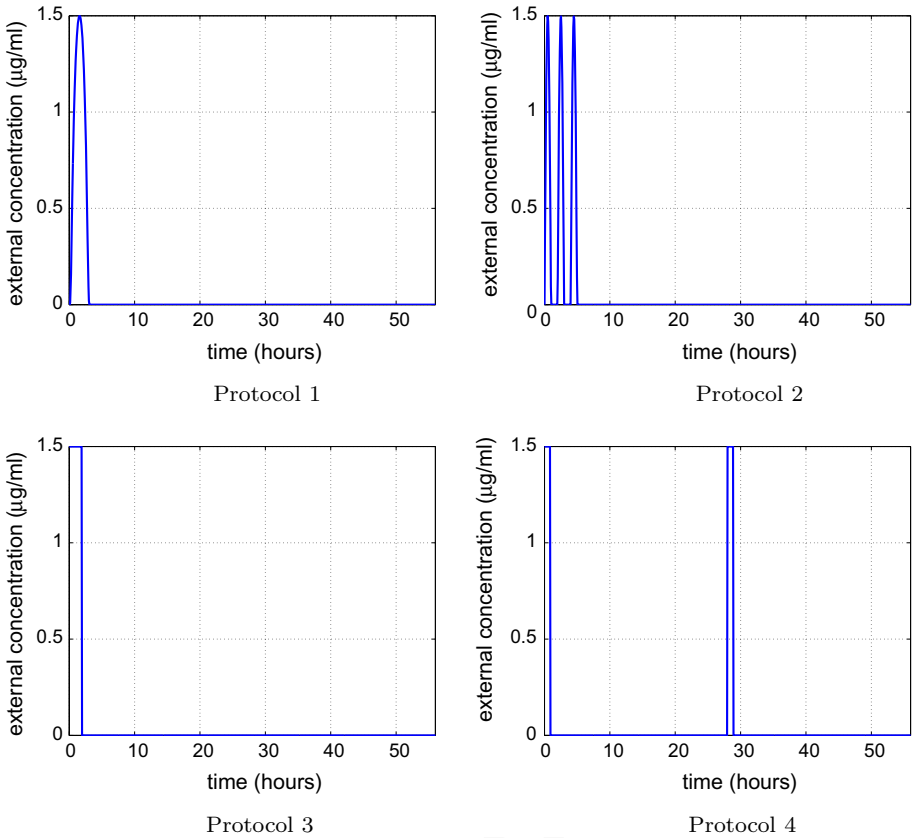


Fig. 1 Possible protocols for drug administration

129
$$n(r, 0) = n_I(r), \quad s(0) = s_I. \tag{6}$$

130 For the boundary conditions, we suppose that there is no flux about $r = 0$ due to symmetry.
 131 The boundary conditions are:

132
$$\begin{aligned} \frac{\partial c}{\partial r}(0, \tau) &= 0, & c(s(\tau), \tau) &= c_0, \\ v(0, \tau) &= 0, & v(s(\tau), \tau) &= s'(\tau), \\ \frac{\partial w}{\partial r}(0, \tau) &= 0, & w(s(\tau), \tau) &= w_0(\tau), \end{aligned} \tag{7}$$

133 where c_0 and $w_0(\tau)$ are external nutrient and drug concentrations, respectively.

134 The function $w_0(\tau)$ depends on the chemotherapy protocol, which describes the schedule
 135 of tests, dosages and the length of the study. For example, we can take different options for
 136 drug administration as shown in Fig. 1. Protocols 3 and 4 represent single and multiple doses
 137 like in (Ward and King 2003), protocols 1 and 2 represent single and multiple doses that
 138 could simulate a more realistic evolution of the external drug concentration.

139 Following the ideas in (Adam 1986; Byrne and Chaplain 1997; Ward and King 1997,
 140 2003), we rescale the mathematical model and transform the spatial domain $[0, s(\tau)]$ of the

141 tumor into the dimensionless spatial interval $[0, 1]$. Similarly, we will define the dimensionless
 142 time t as τA , where the rate A was defined above. This is a very useful approach when dealing
 143 with free boundary problems, as mentioned in (Crank 1984). Hence, let us define the following
 144 functions

$$\begin{aligned}
 145 \quad N(y, t) &= V_L n(y_s(t/A), t/A), \\
 146 \quad C(y, t) &= \frac{1}{c_0} c(y_s(t/A), t/A), \\
 147 \quad V(y, t) &= \frac{1}{Ar_0} v(y_s(t/A), t/A), \\
 148 \quad W(y, t) &= \frac{1}{W_0} w(y_s(t/A), t/A), \\
 149 \quad S(t) &= \frac{1}{r_0} s(t/A),
 \end{aligned} \tag{8}$$

150 where W_0 is a suitable reference drug concentration and $r_0 = (3V_L/(4\pi))^{1/3}$ is the radius of
 151 a single live cell.

152 Notice that if we apply the change of variables (8) to Eqs. (2) and (4), then

$$153 \quad v \left[C_t - \frac{S'}{S} y C_y + \frac{2V}{yS} C + \frac{(VC)_y}{S} \right] = \frac{1}{S^2} \left(C_{yy} + \frac{2}{y} C_y \right) - \widehat{\beta} \widehat{k}_m(C) N, \tag{9}$$

$$\begin{aligned}
 154 \quad \chi \left[W_t - \frac{S'}{S} y W_y + \frac{2V}{yS} W + \frac{(VW)_y}{S} \right] &= \frac{1}{S^2} \left(W_{yy} + \frac{2}{y} W_y \right) \\
 155 \quad &\quad - \frac{\widehat{K}}{\alpha} G(A\widehat{k}_m(C)) W N, \tag{10}
 \end{aligned}$$

156 where

$$157 \quad \widehat{k}_m(C) = \frac{C}{\widehat{c}_c + C},$$

158 and $\nu = Ar_0^2/D$, $\chi = Ar_0^2/D_w$, $\widehat{c}_c = c_c/c_0$, $\widehat{\beta} = Ar_0^2\beta/(V_L c_0 D)$, $\widehat{K} = KW_0/A$ and
 159 $\alpha = \omega D_w W_0 V_L / (Ar_0^2)$.

160 The dimensionless numbers ν and χ can be interpreted as the ratio of two timescales,
 161 namely, the tumor growth ($1/A \approx 1$ day) and the much shorter nutrient and drug diffusions
 162 (r_0^2/D , $r_0^2/D_w \approx 1$ min). Therefore, ν and χ are approximately 10^{-5} . That is why we adopt
 163 a quasi-steady assumption in the nutrient and drug equations [see Ward and King (1997)].

164 Then, the system of Eqs. (1)–(4), taking into account the above comments on Eqs. (9) and
 165 (10), can be written in its nondimensional form as

$$166 \quad N_t - \frac{S'}{S} y N_y + \frac{V}{S} N_y = [a(C, W) - b(C, W)N]N, \tag{11}$$

$$167 \quad C_{yy} + \frac{2}{y} C_y = \widehat{\beta} \widehat{k}_m(C) S^2 N, \tag{12}$$

$$168 \quad V_y + \frac{2}{y} V = b(C, W) S N, \tag{13}$$

$$169 \quad W_{yy} + \frac{2}{y} W_y = \frac{\widehat{K}}{\alpha} G(A\widehat{k}_m(C)) S^2 N W, \tag{14}$$

170 for $0 < y < 1$ and $t > 0$, where

$$\begin{aligned}
 171 \quad \widehat{k}_d(C, W) &= \frac{B}{A} \left(1 - \sigma \frac{C}{\widehat{c}_d + C} \right) + \widehat{K} G(A\widehat{k}_m(C))W, \\
 172 \quad a(C, W) &= \widehat{k}_m(C) - \widehat{k}_d(C, W), \\
 173 \quad b(C, W) &= \widehat{k}_m(C) - (1 - \delta)\widehat{k}_d(C, W),
 \end{aligned}$$

174 and $\widehat{c}_d = c_d/c_0$ and $\delta = V_D/V_L$.

175 The initial and boundary conditions (6)–(7) become:

$$176 \quad N(y, 0) = N_I(y) := V_L n(yS_I, 0), \quad S(0) = \frac{1}{r_0} S_I, \quad (15)$$

177 and

$$\begin{aligned}
 178 \quad C_y(0, t) &= 0, \quad C(1, t) = 1, \\
 V(0, t) &= 0, \quad V(1, t) = S'(t), \\
 W_y(0, t) &= 0, \quad W(1, t) = \frac{1}{w_0} w_0(t/A),
 \end{aligned} \quad (16)$$

179 From now on, Eqs. (11)–(16) will be referred to as the direct problem.

180 3 Solving the direct problem

181 In this section, we will present a numerical scheme for solving the system of Eqs. (11)–(16).
 182 Let n and m be positive integers, $T > 0$ a given final time and consider a uniform space and
 183 time discretization: $y_i = i \Delta y$, $t_j = j \Delta t$, for $i = 0, \dots, n$, and $j = 0, \dots, m$. Then, we
 184 must determine the functional values N_{ij} , C_{ij} , V_{ij} , W_{ij} and S_j satisfying:

$$\begin{aligned}
 185 \quad \frac{N_{i,j+1} - N_{ij}}{\Delta t} - \frac{V_{nj} y_i - V_{ij}}{S_j} \frac{N_{i+1,j} - N_{ij}}{\Delta y} \\
 186 \quad = [a(C_{ij}, W_{ij}) - b(C_{ij}, W_{ij}) N_{ij}] N_{ij}, \quad (17)
 \end{aligned}$$

$$\begin{aligned}
 187 \quad \frac{C_{i+1,j} - 2C_{ij} + C_{i-1,j}}{(\Delta y)^2} + \frac{2}{y_i} \frac{C_{i+1,j} - C_{i-1,j}}{2\Delta y} = \widehat{\beta} \widehat{k}_m(C_{ij}) S_j^2 N_{ij}, \quad (18)
 \end{aligned}$$

$$\begin{aligned}
 189 \quad \frac{V_{i+1,j} - V_{ij}}{\Delta y} + \frac{2}{y_i} V_{ij} = b(C_{ij}, W_{ij}) S_j N_{ij}, \quad (19)
 \end{aligned}$$

$$\begin{aligned}
 190 \quad \frac{W_{i+1,j} - 2W_{ij} + W_{i-1,j}}{(\Delta y)^2} + \frac{2}{y_i} \frac{W_{i+1,j} - W_{i-1,j}}{2\Delta y} = \frac{\widehat{K}}{\alpha} G(A\widehat{k}_m(C_{ij})) S_j^2 N_{ij} W_{ij}, \quad (20)
 \end{aligned}$$

$$\begin{aligned}
 191 \quad \frac{S_{j+1} - S_j}{\Delta t} = V_{nj}. \quad (21)
 \end{aligned}$$

192 Assuming that functions N , C , V , W , and S are sufficiently smooth, we can avoid the
 193 singularity of (12)–(14) at $y = 0$. Notice that $C_y(0, t) = 0$ [by (16)] implies $C_y(y, t)/y \rightarrow$
 194 $C_{yy}(0, t)$ when $y \rightarrow 0$. Analogously, for V and W , we obtain

$$\begin{aligned}
 195 \quad 3C_{yy}(0, t) &= \widehat{\beta} \widehat{k}_m(C(0, t)) S(t)^2 N(0, t), \\
 196 \quad 3V_y(0, t) &= b(C(0, t), W(0, t)) S(t) N(0, t), \\
 197 \quad 3W_{yy}(0, t) &= \frac{\widehat{K}}{\alpha} G(A\widehat{k}_m(C(0, t))) S(t)^2 N(0, t) W(0, t).
 \end{aligned}$$

Discretizing the above equations, we have

$$6 \frac{C_{1j} - C_{0j}}{(\Delta y)^2} = \widehat{\beta} \widehat{k}_m(C_{0j}) S_j^2 N_{0j}, \quad (22)$$

$$6 \frac{W_{1j} - W_{0j}}{(\Delta y)^2} = \frac{\widehat{K}}{\alpha} G(A \widehat{k}_m(C_{0j})) S_j^2 N_{0j} W_{0j}, \quad (23)$$

$$3 \frac{V_{1j}}{\Delta y} = b(C_{0j}, W_{0j}) S_j N_{0j}, \quad (24)$$

where we used a central difference on space at the boundary $y = 0$ to obtain $C_{yy}(0, t_j) \approx 2(C_{1j} - C_{0j})/(\Delta y)^2$ (similarly for variables W and V).

On the other hand, by Eq. (17) and using the fact that $y_n = 1$ and $C_{nj} = 1$ for all j , we get

$$\frac{N_{n,j+1} - N_{nj}}{\Delta t} = [a(1, W_{nj}) - b(1, W_{nj}) N_{nj}] N_{nj}, \quad (25)$$

The procedure for solving the discretized Eqs. (17)–(25) is the following.

Algorithm 1

1. Set $j = 0$.
2. If $j = 0$ set $N_{i0} = N_I(y_i)$ for $i = 0, \dots, n$, and $S_0 = s_I/r_0$, otherwise
 - Define N_{nj} satisfying Eq. (25).
 - Define N_{ij} , $i = 0, \dots, n - 1$ satisfying (17).
 - Define S_j satisfying (21).
3. Set $C_{nj} = 1$ and find C_{ij} , $i = 0, \dots, n - 1$ solving the nonlinear system (18) and (22).
4. Set $W_{nj} = w_0(t_j)/W_0$ and find W_{ij} , $i = 0, \dots, n - 1$ solving the linear system (20) and (23).
5. Set $V_{0j} = 0$ and find V_{ij} , $i = 1, \dots, n$ solving the linear system (19) and (24).
6. Set $j = j + 1$ and return to step 2.

To verify the numerical procedure, we solved the direct problem (11)–(16) associated to a real tumor. Let us consider V79 spheroids growing in glucose supply conditions. This cell line, which was developed from lung tissue of a young male Chinese hamster, has a high plating efficiency (80%), and a generation time of 12–14h. The line was renamed V79 by Elkind in 1958 (Ford et al. 1958).

According to (Hlatky et al. 1988; Ward and King 1997, 2003) and references therein, the corresponding parameters are: $c_c = 1.4 \times 10^{-4}$ g/cm³, $c_d = 7 \times 10^{-5}$ g/cm³, $A = B = 1.98 \times 10^{-5}$ 1/s, $\sigma = 0.9$, $K = 661.39$ cm³/(gs), $D = 1.1 \times 10^{-6}$ cm²/s, $\beta = 1.01 \times 10^{-9}$ g/cell, $V_L = 10^{-9}$ cm³, $V_D = 5 \times 10^{-10}$ cm³, $D_w = 5.5 \times 10^{-6}$ cm²/s and $c_0 = 1.4 \times 10^{-3}$ g/cm³. Consequently, the dimensionless parameters corresponding to the direct problem are: $\widehat{c}_c = 0.1$, $\widehat{c}_d = 0.05$, $\widehat{K} = 50$, $\widehat{\beta} = 0.005$, $\delta = 0.5$. We assume a linear dependence between drug action and cell cycle, that is, $G(k_m(c)) = k_m(c)/A$ (Ward and King 2003).

If we first consider the tumor growth without the action of the drug, beginning from a single cell, we can see that the evolution of the radius is linear with respect to time for large times (see Fig. 2a). In Fig. 2b, we also show the evolution of the live cell density and the growth of the necrotic core. Thus, the resolution of the proposed numerical scheme, removing the action of the drug, is compatible with the results presented in (Ward and King 1997, Figs. 1, 2).

Now, let the tumor evolve without the action of the drug from a dimensionless time equal to -25 (corresponding to 350h) obtaining a tumor size of $S(0) = 141.87$ (corresponding

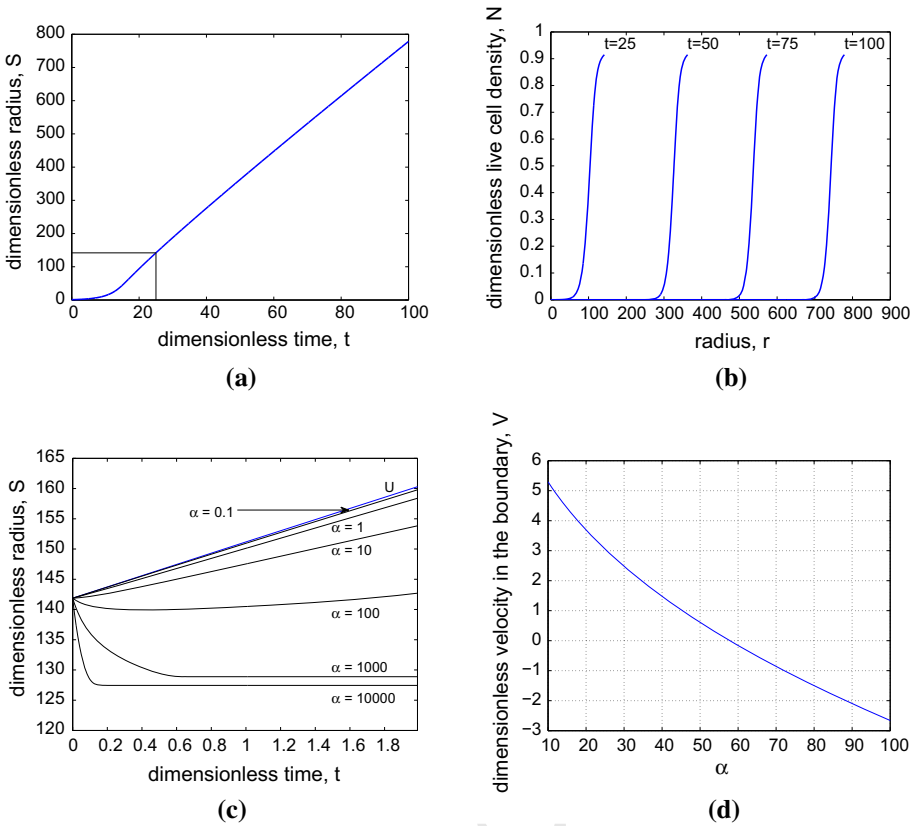


Fig. 2 a, b show the evolution of the tumor radius and the live cell density without the action of drug. c shows the evolution of the tumor radius under a chemotherapy treatment for several values of α . d Velocity at the tumor’s boundary for a fixed dimensionless time ($t = 0.2$) for different values of α

239 to 880.9 μm) and an initial live cell density $N_I(y)$. From that moment, we apply a protocol
 240 consisting of a 28 h exposure to a constant drug concentration $w_0(\tau) = 1.5 \mu\text{g/ml}$, $0 \leq \tau \leq$
 241 28. We solved the direct problem for several values of the parameter α as shown in Fig. 2c
 242 obtaining results similar to those in (Ward and King 2003, Fig. 2). From Fig. 2c, we can see
 243 that the parameter α can be regarded as the dimensionless effectiveness of the drug since for
 244 greater values of α the tumor becomes smaller (see the definition of α).

245 An interesting question to answer is: *for which value of α can be stated that tumor will*
 246 *decrease in size?* To determine this value, we take into account the velocity in the boundary
 247 at a fixed time for different values of α . For example, in Fig. 2d, we can see that if we fix the
 248 dimensionless time $t = 0.2$, the function $V(1, t)$ has a root in $\alpha \approx 58$.

249 4 Inverse problem

250 As it was mentioned before, some of the parameters that describe the mathematical model
 251 are unknown, for example, $c_c, c_d, A, B, \sigma, \omega$, among others. However, for parameters related
 252 to the model without the action of the drug (Ward and King 1997), it is not necessary to

consider the model described in (Ward and King 2003). For a methodology for estimating those parameters, we refer to (Knopoff et al. 2013). In this work, we focused on the recovery of the parameter α since it appears exclusively in the model with drug and it represents its dimensionless effectiveness. Moreover, it can be shown that the drug penetration depth is equal to $r_0(\alpha/\hat{K})^{1/2}$. For this purpose, we formulate the following problem:

Find a parameter value α^ able to generate data that best match the available information over time $0 \leq t \leq T$.*

Since the direct problem can be solved for each value of $\alpha > 0$, we should construct an objective function \mathcal{J} which gives us some *distance* between the experimental (real) data and the solution of the direct problem for each value of α . Thus, the inverse problem can be formulated as:

$$\text{Find } \alpha^* > 0 \text{ such that } \mathcal{J}(\alpha^*) \leq \mathcal{J}(\alpha) \text{ for all } \alpha > 0, \quad (26)$$

or equivalently

$$\alpha^* = \underset{\alpha > 0}{\operatorname{argmin}} \mathcal{J}(\alpha). \quad (27)$$

To define a suitable objective function \mathcal{J} , it is important to decide which variables could be measured experimentally, for instance, the tumor radius evolution. So, the first possibility for defining a function (associated to the dimensionless problem) could be

$$\mathcal{J}(\alpha) = \int_0^T (S_\alpha(t) - S^*(t))^2 dt, \quad (28)$$

where $S_\alpha(t)$ is the dimensionless radius at time t obtained by solving the direct problem for a certain value of α , and $S^*(t)$ is a function that is obtained (e.g., by interpolation) from experimental measurements of the the tumor radius at certain times.

Motivated by the considerations stated in (Ward and King 2003, pp. 194–196) based on (Sano et al. 1984): “...there is very little difference in cell survival, at the time the final treatment ends, between a single dose of the drug or the same amount of drug applied in multiple doses”, we define a function representing the mean external drug concentration over the duration of the experiment, namely:

$$\mathcal{I}(w_o) = \frac{1}{\tilde{\tau}} \int_0^{\tilde{\tau}} w_o(\tau) d\tau, \quad (29)$$

where $\tilde{\tau}$ is the dimensional final time ($\tilde{\tau} = T/A$). Note that \mathcal{I} is a quantity that depends on the drug administration protocol and that it has units corresponding to concentration.

The four protocols shown in Fig. 1 were selected in such a way that the quantity \mathcal{I} is conserved for all of them. From Fig. 3, we observe that after drug treatment with these protocols, the spheroids recover to grow at comparable sizes.

Thus, it is reasonable to consider an objective function that takes into account only the tumor radius at final time, that is

$$\mathcal{J}(\alpha) = (S_\alpha(T) - S^*(T))^2. \quad (30)$$

where S_α can be obtained from any protocol with the same \mathcal{I} associated to the protocol used to obtain the data S^* .

Finally, if it were possible to have measurements of the live cell density inside the tumor for certain times, we could define:

$$\mathcal{J}(\alpha) = \mu \int_0^1 \int_0^T (N_\alpha(y, t) - N^*(y, t))^2 dt dy + \int_0^T (S_\alpha(t) - S^*(t))^2 dt, \quad (31)$$

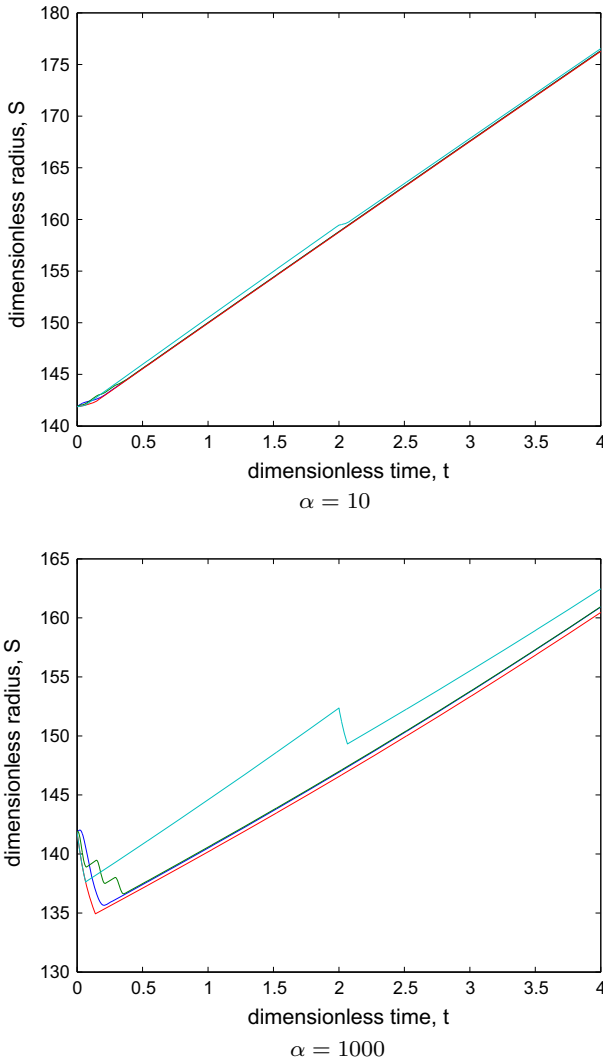


Fig. 3 Evolution of the tumor radius for different treatment protocols: **a** blue for protocol 1, **b** green for protocol 2, **c** red for protocol 3 and **d** cyan for protocol 4

293 where N_α is the dimensionless live cell density obtained by solving the direct problem for a
 294 certain value of α , N^* is a function that is obtained (e.g., by interpolation) from experimental
 295 measurements of the the live cell density, and μ is a scaling parameter. Notice that when
 296 $\mu = 0$, we recover the objective function as in (28).

297 We have defined the objective functions in terms of variables that can be experimentally
 298 measured as explained in Knopoff et al. (2013). For example, the density of living cells
 299 could be measured via biomedical imaging like PET technique for a tumor in vivo, or via
 300 immunofluorescence and electronic scan microscopy technique for in vitro cases (Taylor et al.
 301 1986; Martin et al. 1994). In addition, in (Freyer et al. 1986), the mean size of a spheroid
 302 population was determined by measuring two orthogonal diameters on spheroids using an

inverted microscope fitted with a calibrated eyepiece reticule. Also, in (Monazzam et al. 2007; Bergstrom et al. 2008), a special procedure was used with digital microscope photos to evaluate tumor growth. Finally, in (Herrmann et al. 2008), spheroids were photographed in an inverted phase contrast microscope while a micrometer scale was photographed at the same magnification, and spheroid size was determined.

Advantages and disadvantages of each objective function will become clear later.

5 Numerical experiments

To solve the inverse problem (26), we used a Pattern Search method (Torczon 1997; Dolan et al. 2003; Audet and Dennis 2002). This method is a very effective numerical optimization method for engineering problems where the computation of the derivative of the objective function is expensive. In particular, it belongs to the family of derivative-free methods.

Pattern Search methods proceed by conducting a series of exploratory moves about the current iterate before identifying a new iterate. These moves can be viewed as a search about the current iterate for a trial point with a lower function value. At each iteration, the algorithm reduces the step size if the exploratory moves algorithm fails to produce a trial step that gives a simple decrease. If the exploratory moves algorithm does produce a trial step that gives a simple decrease, then this algorithm either increases the step size or preserves the current step size. An implementation of this method can be found in (Venkataraman 2009).

The numerical experiments were run in Matlab R2011a in a PC running Linux OS, Intel Core i5. The direct problem was solved according to Algorithm 1 with parameters $m = 800$, $n = 500$, $T = 4$; initial conditions S_0 and N_I were obtained after letting the tumor evolve without the action of the drug from a dimensionless time equal to -25 ; physical constants correspond to a V79 spheroid growing in glucose supply conditions. The inverse problem was solved using the Matlab built-in function `patternsearch` with an initial point randomly chosen in the interval $[0, 10^6]$. Function (28) was computed employing the composite trapezoidal rule with temporal discretization taken as in the direct problem. The function S_α in (30) was calculated using protocol 3 for all the experiments.

Consider first the optimization problem (26) that consists of minimizing the functions (28) or (30), where S^* is generated by solving the direct problem using Algorithm 1, for certain choices of the model parameter $\alpha = \alpha^*$, where $\alpha^* = 17.3$, $\alpha^* = 314.0$ and $\alpha^* = 5350.1$, to represent different orders of magnitude that this parameter can attain. We perform these simulations for the four protocols shown in Fig. 1. Then, to study the stability of the proposed procedure, we consider a tumor radius measurement affected with a random noise of $\pm 5 \mu\text{m}$ uniformly distributed, that for the considered spheroids corresponds to about 0.5 % of the tumor radius. The noise was generated using the Matlab built-in function `rand`.

We perform some experiments to investigate how close the original value of the parameter can be retrieved. We stress that the inverse problem is not trivial, because we do not know, for instance, if the optimization problem has a solution or, in that case, if it is unique or if the method converges to another local minima. However, according to Fig. 4, the shape of the objective functions indicates that the inverse problem (26) has a unique solution.

Tables 2, 3, 4 and 5 show the solution of the inverse problem for certain protocols and certain values of α^* .

On one hand, according to Table 2, the estimated parameter α is retrieved very well, with a percent error lower than 0.4 % in most cases, using the function (28) for every choice of α^* . On the other hand, Table 3 shows that the parameter α is retrieved quite well for large values

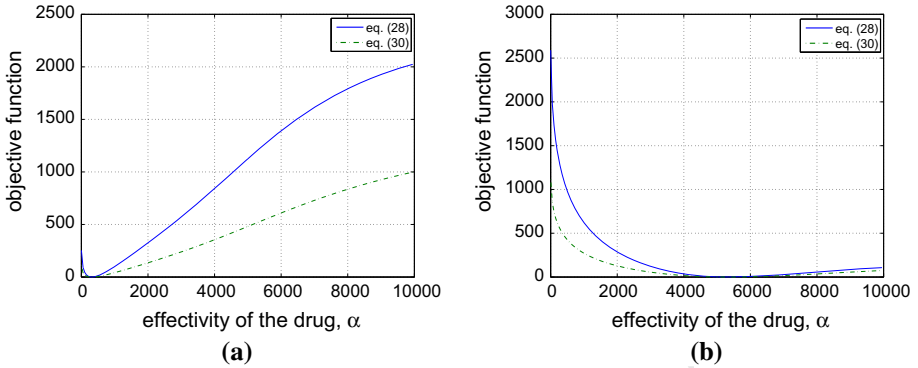


Fig. 4 Objective functions (28) and (30) for $\mathbf{a} \alpha^* = 314$ and $\mathbf{b} \alpha^* = 5350.1$

Table 2 Estimated α and percent error $e\%$ with function (28) using generated data without noise

α^*	Protocol 1		Protocol 2		Protocol 3		Protocol 4	
	α_{est}	$e\%$	α_{est}	$e\%$	α_{est}	$e\%$	α_{est}	$e\%$
17.3	17.23	0.39	17.27	0.17	17.81	2.97	16.53	4.48
314.0	313.24	0.24	313.60	0.13	314.58	0.18	314.54	0.17
5350.1	5349.12	0.02	5351.03	0.02	5349.24	0.02	5349.46	0.01

Table 3 Estimated α and percent error $e\%$ with function (28) using generated data with noise

α^*	Protocol 1		Protocol 2		Protocol 3		Protocol 4	
	α_{est}	$e\%$	α_{est}	$e\%$	α_{est}	$e\%$	α_{est}	$e\%$
17.3	24.83	43.52	10.48	39.44	22.95	32.68	8.05	53.46
314.0	329.87	5.05	286.32	8.82	349.86	11.42	268.30	14.56
5350.1	5195.90	2.88	5374.20	0.45	5128.40	4.14	5198.70	2.83

Table 4 Estimated α and percent error $e\%$ with function (30) using generated data without noise

α^*	Protocol 1		Protocol 2		Protocol 3		Protocol 4	
	α_{est}	$e\%$	α_{est}	$e\%$	α_{est}	$e\%$	α_{est}	$e\%$
17.3	15.92	7.98	17.27	0.19	18.05	4.32	13.24	23.49
314.0	295.24	5.98	295.24	5.98	313.69	0.10	241.93	22.95
5350.1	4918.20	8.07	4755.00	11.12	5349.60	0.01	3257.60	39.11

348 of α^* . To recover small values of α^* , it is necessary to have more accurate measurements.
 349 Notice that in the experiments with and without noise, the percent error decreases as α^*
 350 becomes greater.

351 Since we need to compute a good approximation of the integral in (28), it is necessary to
 352 have enough measurements to capture the tumor’s evolution for a given protocol.

Table 5 Estimated α and percent error $e\%$ with function (30) using generated data with noise

α^*	Protocol 1		Protocol 2		Protocol 3		Protocol 4	
	α_{est}	$e\%$	α_{est}	$e\%$	α_{est}	$e\%$	α_{est}	$e\%$
17.3	16.72	3.34	14.63	15.43	32.67	88.83	3.26	81.18
314.0	352.54	12.27	291.45	7.18	310.56	1.10	182.93	41.74
5350.1	4824.10	9.83	4981.00	6.90	5360.90	0.20	3280.70	38.68

353 If it were not possible to have measurements of the tumor radius for several times, or if the
 354 drug administration protocol were unknown, we could use the function (30) that requires only
 355 a measurement at final time and an estimation of the mean external drug concentration value
 356 \mathcal{I} [see (29)]. It is observed that the results obtained using this function are, although worse
 357 than those from function (28), still acceptable, given the limited information required. If this
 358 information is affected with noise, then it will clearly be a source of errors, so more accurate
 359 measurements are needed. Tables 4 and 5 show that, in general, the percent errors are around
 360 10 % for protocols 1 and 2. Protocol 3 is remarkably good compared with the other protocols
 361 in most cases, maybe due to the fact that the function S_α in (30) was obtained precisely
 362 with this protocol. Results in protocol 4 are not satisfactory at all, maybe due to an early
 363 final observation time. For example, notice from Fig. 3 that the furthest curve corresponds to
 364 protocol 4. This curve has not yet reached its stationary behavior, so a larger final time must
 365 be considered.

366 6 Conclusions and looking ahead

367 A methodology for the estimation of the drug effectiveness parameter, which is involved in the
 368 growth of an avascular in vitro tumor with drug, has been presented in this paper. Basically,
 369 we used the Pattern Search method to solve the inverse problem that can be regarded as
 370 a PDE-constrained optimization problem, where the constraints are given by the coupled
 371 system of PDEs proposed by Ward and King (2003).

372 Two objective functions were proposed to solve the inverse problem. The first one takes
 373 into account the evolution of the tumor radius on time. It is worth stressing that the numerical
 374 experiments performed with this function let us retrieve the parameter α accurately, especially
 375 for the cases in which no noise was added to the data. The counterpart is that the radius should
 376 be monitored at various times and that the drug administration protocol should be known. The
 377 second objective function only needs one measurement of the radius at a final time and the
 378 knowledge of the mean external drug concentration during the simulation time. Of course,
 379 the cost of using less information is that the parameter is retrieved with a higher, but still
 380 acceptable, error.

381 There is considerable scope for further work and future research based on the approach
 382 presented in this paper. For instance, an obvious extension is to consider a more complex
 383 model for an in vitro tumor representing the vascularized case. The following step could be
 384 to move on to the in vivo case where parameters are even more difficult to retrieve, either
 385 by the intrinsic complexity of the model or by the lack of suitable measurements. The same
 386 reasonings apply to the case of the growth of cancer cells under the surveillance of the
 387 immune system, for instance in Bellouquid et al. (2013), a qualitative analysis is performed
 388 but it would be worth retrieving the parameters accurately to validate the model.

389 **Acknowledgments** We thank the referees and the Editor for their careful reading of the manuscript and their
 390 valuable suggestions. This work was carried out with the aid of grants from ANPCyT, CONICET and SECyT-
 391 UNC; and the European Union FP7 Health Research Grant No. FP7-HEALTH-F4-2008-202047-RESOLVE.

392 References

- 393 Adam JA (1986) A simplified mathematical model of tumor growth. *Math Biosci* 81(2):229–244
 394 Agnelli J, Barrea A, Turner C (2011) Tumor location and parameter estimation by thermography. *Math Comput*
 395 *Model* 53(7–8):1527–1534
 396 Audet C, Dennis J (2002) Analysis of generalized pattern searches. *SIAM J Optimiz* 13(3):889–903
 397 Bellomo N, Li N, Maini P (2008) On the foundations of cancer modelling: selected topics, speculations, and
 398 perspectives. *Math Model Methods Appl Sci* 18(4):593–646
 399 Bellouquid A, De Angelis E, Knopoff D (2013) From the modeling of the immune hallmarks of cancer to a
 400 black swan in biology. *Math Model Methods Appl Sci* 23(05):949–978
 401 Bergstrom M, Monazzam A, Razifar P, Ide S, Josephsson R, Langstrom B (2008) Modeling spheroid growth,
 402 PET tracer uptake, and treatment effects of the Hsp90 inhibitor NVP-AUY922. *J. Nucl. Med.* 49(7):1204–
 403 1210
 404 Byrne H, Chaplain M (1997) Free boundary value problems associated with the growth and development of
 405 multicellular spheroids. *Eur J Appl Math* 8(06):639–658
 406 Byrne H, Drasdo D (2009) Individual-based and continuum models of growing cell populations: a comparison.
 407 *J Math Biol* 58:657–687
 408 Crank J (1984) Free and moving boundary problems. Oxford Science Publications, The Clarendon Press,
 409 Oxford University Press, New York
 410 Dolan E, Lewis R, Torczon V (2003) On the local convergence of pattern search. *SIAM J Optimiz* 14(2):567–
 411 583
 412 Edelman LB, Eddy JA, Price ND (2010) In silico models of cancer. *WIREs Syst Biol Med* 2(4):438–459
 413 Ford DK, Yerganian G (1958) Observations on the chromosomes of Chinese hamster cells in tissue culture. *J*
 414 *Natl Cancer Inst* 21(2):393–425
 415 Freyer JP, Sutherland RM (1986) Regulation of growth saturation and development of necrosis in EMT6/Ro
 416 multicellular spheroids by the glucose and oxygen supply. *Cancer Res* 46(7):3504–3512
 417 Greenspan H (1972) Models for the growth of a solid tumor by diffusion. *Stud Appl Math* 51(4):317–340
 418 Grillo A, Wittum G, Giaquinta G, Mićunović MV (2009) A multiscale analysis of growth and diffusion
 419 dynamics in biological materials. *Int J Eng Sci* 47(2):261–283
 420 Hamilton G (1998) Multicellular spheroids as an in vitro tumor model. *Cancer Lett* 131(1):29–34
 421 Herrmann R, Fayad W, Schwarz S, Berndtsson M, Linder S (2008) Screening for compounds that induce
 422 apoptosis of cancer cells grown as multicellular spheroids. *J Biomol Screen* 13(1):1–8
 423 Hlatky L, Sachs RK, Alpen EL (1988) Joint oxygen-glucose deprivation as the cause of necrosis in a tumor
 424 analog. *J Cell Physiol* 134(2):167–178
 425 Hogeia C, Davatzikos C, Biros G (2008) An image-driven parameter estimation problem for a reaction-diffusion
 426 glioma growth model with mass effects. *J Math Biol* 56(6):793–825
 427 Kiran KL, Jayachandran D, Lakshminarayanan S (2009) Mathematical modelling of avascular tumour growth
 428 based on diffusion of nutrients and its validation. *Can J Chem Eng* 87(5):732–740
 429 Knopoff D, Fernández D, Torres G, Turner C (2013) Adjoint method for a tumor growth PDE-constrained
 430 optimization problem. *Comput Math Appl* 66(6):1104–1119
 431 Lowengrub J, Frieboes H, Jin F, Chuang Y, Li X, Macklin P, Wise S, Cristini V (2010) Nonlinear modelling
 432 of cancer: bridging the gap between cells and tumours. *Nonlinearity* 23:R1
 433 Martin GR, Jain RK (1994) Noninvasive measurement of interstitial pH profiles in normal and neoplastic
 434 tissue using fluorescence ratio imaging microscopy. *Cancer Res* 54(21):5670–5674
 435 Monazzam A, Josephsson R, Blomqvist C, Carlsson J, Langstrom B, Bergstrom M (2007) Application of the
 436 multicellular tumour spheroid model to screen PET tracers for analysis of early response of chemotherapy
 437 in breast cancer. *Breast Cancer Res* 9(4):R45
 438 Oden JT, Prudencio EE, Hawkins-Daarud A (2013) Selection and assessment of phenomenological models of
 439 tumor growth. *Math Model Methods Appl Sci* 23(07):1309–1338
 440 Perthame B, Zubelli JP (2007) On the inverse problem for a size-structured population model. *Inverse Probl*
 441 23(3):1037–1052
 442 Preziosi L, Vitale G (2011) A multiphase model of tumor and tissue growth including cell adhesion and plastic
 443 reorganization. *Math Model Methods Appl Sci* 21(09):1901–1932

- 444 Rejniak K, McCawley L (2010) Current trends in mathematical modeling of tumor-microenvironment inter-
445 actions: a survey of tools and applications. *Exp Biol Med* 235(4):411–423
- 446 Roose T, Chapman S, Maini P (2007) Mathematical models of avascular cancer. *SIAM Rev* 49(2):179–208
- 447 Sano Y, Hoshino T, Barker M, Deen DF (1984) Response of 9L rat brain tumor multicellular spheroids to
448 single and fractionated doses of 1,3-bis (2-chloroethyl)-1-nitrosourea. *Cancer Res* 44(2):571–576
- 449 Sutherland R (1988) Cell and environment interactions in tumor microregions: the multicell spheroid model.
450 *Science* 240(4849):177–184
- 451 Taylor DL, Waggoner AS, Lanni F, Murphy RF, Birge RR (1986) Applications of fluorescence in the biomedical
452 sciences. Alan R, Liss Inc, Technical Report
- 453 Torczon V (1997) On the convergence of pattern search algorithms. *SIAM J Optimiz* 7(1):1–25
- 454 Tracqui P (2009) Biophysical models of tumour growth. *Rep Prog Phys* 72:056701
- 455 van den Doel K, Ascher UM, Pai DK (2011) Source localization in electromyography using the inverse
456 potential problem. *Inverse Probl* 27(2):025008
- 457 Venkataraman P (2009) Applied optimization with MATLAB programming. Wiley, London
- 458 Ward J, King J (1997) Mathematical modelling of avascular-tumour growth. *Math Med Biol* 14(1):39–69
- 459 Ward JP, King JR (2003) Mathematical modelling of drug transport in tumour multicell spheroids and mono-
460 layer cultures. *Math Biosci* 181(2):177–207
- 461 Wise S, Lowengrub J, Frieboes H, Cristini V (2008) Three-dimensional multispecies nonlinear tumor growth-I:
462 model and numerical method. *J Theor Biol* 253(3):524–543
- 463 Zubelli JP, Marabini R, Sorzano COS, Herman GT (2003) Three-dimensional reconstruction by chahine's
464 method from electron microscopic projections corrupted by instrumental aberrations. *Inverse Probl*
465 19(4):933–949

Journal: 40314
Article: 259

Author Query Form

**Please ensure you fill out your response to the queries raised below
and return this form along with your corrections**

Dear Author

During the process of typesetting your article, the following queries have arisen. Please check your typeset proof carefully against the queries listed below and mark the necessary changes either directly on the proof/online grid or in the 'Author's response' area provided below

Query	Details required	Author's response
1.	As per the information provided by the publisher, Fig. 3 will be black and white in print; hence, please confirm whether we can add "colour figure online" to the caption.	